



Published in final edited form as:

Hypertension. 2012 June ; 59(6): 1170–1178. doi:10.1161/HYPERTENSIONAHA.111.186072.

Left ventricular failure produces profound lung remodeling and pulmonary hypertension in mice: heart failure causes severe lung disease

Yingjie Chen¹, Haipeng Guo^{1,2,*}, Dachun Xu^{1,3,*}, Xin Xu¹, Huan Wang¹, Xinli Hu¹, Zhongbing Lu¹, Dongmin Kwak¹, Yawei Xu³, Roland Gunther⁴, Yuqing Huo¹, and E. Kenneth Weir⁵

¹Lillehei Heart Institute and the Cardiovascular Division, University of Minnesota Medical School, Minneapolis, Minnesota

²Key Laboratory of Cardiovascular Remodeling and Function Research, Qilu Hospital, Shandong University, Shandong, China

³Department of Cardiology, Shanghai Tenth People's Hospital, of Tongji University, Shanghai, China

⁴Research Animal Resources, University of Minnesota Minneapolis, Minnesota

⁵Department of Medicine, University of Minnesota and Veterans Affairs Medical Center, Minneapolis, Minnesota

Abstract

Chronic left ventricular failure causes pulmonary congestion with increased lung weight and type-2 pulmonary hypertension. Understanding the molecular mechanisms for type-2 pulmonary hypertension and the development of novel treatments for this condition requires a robust experimental animal model and a good understanding of the nature of the resultant pulmonary remodeling. Here we demonstrate that chronic transverse aortic constriction causes massive pulmonary fibrosis and remodeling, and type-2 pulmonary hypertension in mice. Thus, aortic constriction-induced left ventricular dysfunction and increased left ventricular end-diastolic pressure is associated with up to 5.3-fold increase in lung wet weight and dry weight, pulmonary hypertension and right ventricular hypertrophy. Interestingly, the aortic constriction-induced increase in lung weight was not associated with pulmonary edema, but resulted from profound pulmonary remodeling with a dramatic increase in the percentage of fully muscularized lung vessels, marked vascular and lung fibrosis, myofibroblast proliferation, and leukocyte infiltration. The aortic constriction-induced left ventricular dysfunction was also associated with right ventricular hypertrophy, increased right ventricular end-diastolic pressure and right atrial hypertrophy. The massive lung fibrosis, leukocyte infiltration and pulmonary hypertension in mice after transverse aortic constriction clearly indicate that congestive heart failure also causes severe lung disease. The lung fibrosis and leukocyte infiltration may be important mechanisms in the poor clinical outcome in patients with end-stage heart failure. Thus, the effective treatment of left

Correspondence: Yingjie Chen, MD, PhD Lillehei Heart Institute & Cardiovascular Division University of Minnesota 420 Delaware Street SE Minneapolis, MN 55455 Tel: 612-624-8970; Fax: 612-626-4411 chenx106@umn.edu.

*These authors contributed equally to this work.

Disclosures None.

Publisher's Disclaimer: This is a PDF file of an unedited manuscript that has been accepted for publication. As a service to our customers we are providing this early version of the manuscript. The manuscript will undergo copyediting, typesetting, and review of the resulting proof before it is published in its final citable form. Please note that during the production process errors may be discovered which could affect the content, and all legal disclaimers that apply to the journal pertain.

ventricular failure may require additional efforts to reduce lung fibrosis and the inflammatory response.

Keywords

pulmonary hypertension; transverse aortic constriction; pulmonary vascular morphology

Introduction

Pulmonary hypertension (**PH**) secondary to left ventricular systolic or diastolic dysfunction or to valvular disease is classified as type-2 PH.¹ The occurrence of PH in the setting of elevated left atrial pressure (pulmonary venous hypertension) has been recognized since the 1940's. In 1945, Andre Cournand et al published the pulmonary artery pressure trace in a case of "rheumatic valvulitis with hypertension in the lesser circulation".² The pulmonary artery systolic pressure was over 80mmHg. It is predicted that up to 60% of patients with severe left ventricular (**LV**) systolic dysfunction and up to 70% of patients with LV diastolic dysfunction may develop PH, but the detailed pulmonary remodeling in type-2 PH is not well defined. The presence of PH in these patients is associated with a worse prognosis.³⁻⁶ In view of the growing prevalence of LV systolic and diastolic failure, the clinical importance of type-2 PH is becoming more prominent. Here we report a dramatic increase of lung weight, massive pulmonary fibrosis, leukocyte infiltration, profound vascular remodeling, type-2 PH and right ventricular dysfunction in mice in response to LV systolic pressure overload produced by chronic transverse aortic constriction (TAC). However, the marked increase of lung weight four weeks post-TAC in mice with severe LV dysfunction was not the result of an increase of lung water content. Our findings suggest that the effective treatment of LV end-stage heart failure may also require additional efforts to reduce lung fibrosis and the inflammatory response.

Materials and Methods

Please see <http://hyper.ahajournals.org> for the detailed Methods.

Experimental animals

C57B6J (Jackson Laboratory) mice were used for the described studies. This study was approved by the Institutional Animal Care and Use Committee of University of Minnesota. Study was conducted in accordance with the National Institutes of Health Guide for the Care and Use of Laboratory Animals.

Induction of PAH with TAC or hypoxia in mice

Male mice at age 10–14 weeks were used for the minimally invasive TAC procedure as we have previously described.⁷⁻¹⁰ For induction of PAH with hypoxia, mice were exposed to hypobaric hypoxia.⁹

Sample Preparation

Heart, lung, and other major organs were harvested and weighed. The ratio of RV weight to left ventricle (LV) + septum (S) was calculated as an index of RV hypertrophy.^{9, 11} The airways of the upper right lobe were perfused and fixed in 10% buffered formalin for histological analysis. Visual comparable inflation of the lung lobes were observed in all tissues.

Measure lung water content and RT-PCR

Lung (lower right lobe) wet weight was first determined. The lung tissue was then dried at 58°C to a constant weight. The dry weight of lung tissue was then determined. The relative water content of lung tissue was calculated using the following equation: Lung water content = (lung wet weight – lung dry weight)/lung wet weight × 100%.

The sequences of the primers used for quantitative real-time PCR are provided in Table S1.

Results

The TAC-induced increases of lung weight and RV hypertrophy are related to the degree of LV failure

Previous studies demonstrated that TAC-induced LV hypertrophy and LV dysfunction are associated with increases in lung weight,^{8,9,12,13} left atrial weight⁸ and RV weight. However, no study has carefully investigated the relationships of these parameters. To further understand the cardiac and pulmonary changes occurring secondary to LV dysfunction, we determined the relationships of LV hypertrophy, LV dysfunction, and increases of left atrial weight, lung weight and RV weight in a group of mice after moderate TAC-induced LV hypertrophy and dysfunction. As demonstrated in Figure 1, the increases of LA weight, lung weight, RV weight and their ratio to body weight after TAC are significantly related to the increase of LV weight or its ratio to bodyweight in these mice, but their relationships are in a nonlinear fashion (Figure 1A–C). However, the decrease of LV ejection fraction was correlated to the increase of the ratio of LV weight to bodyweight in a largely linear fashion (Figure 1D). The increase of LA weight, lung weight, RV weight and their ratio to bodyweight after TAC are all significantly correlated to the decrease of LV ejection fraction (Figure 1E–G). Increase of the ratio of RV weight to bodyweight (a reliable marker for pulmonary hypertension) was also correlated to the increase of the ratio of lung weight to body weight in a nonlinear fashion (Figure 1H).

TAC-induced severe LV dysfunction is an effective cause of increases in lung weight, PA and RV hypertrophy in mice

To further determine whether the degree of LV failure affects the severity of TAC-induced lung remodeling and RV hypertrophy, mice after TAC were divided into a severe LV failure group (**HF**, when LV ejection fraction is less than 50%), or mild/moderate heart failure group (**M-HF**, when LV ejection fraction is greater than 50%). The data obtained from these groups were further compared with the data obtained from a group of control C57B6J mice (control, or Ctr) and a group of C57B6J mice subjected to 3 weeks of hypoxia (Hypoxia) (Figure 2, Table S1). As shown in Figure 2, hypoxia causes no LV dysfunction, and no LV or LA hypertrophy, but did cause a small but significant increase in the ratio of lung weight to body weight, and approximately 50% RV hypertrophy. HF and M-HF mice had decreased LV ejection fraction, 42.7±1.85% and 66.2±3.42%, respectively (Control LV ejection fraction was 80.1±1.07%) (Figure 2A). Both HF and M-HF mice had significant LV hypertrophy, LA hypertrophy, and a significant increase in the ratio of lung weight to body weight (Figure 2B–D), although these increases were significantly greater in the HF group. Interestingly, all of the HF mice had an increase of lung weight above 50%, while only one of twelve M-HF mouse had lung weight increased over 50%, indicating that lung weight is a highly reliable marker for LV dysfunction. The M-HF group had no RV hypertrophy and a minimal increase of lung weight, while the HF group had a dramatic increase of lung weight and significant RV hypertrophy (Figure 2D, E). Neither the hypoxia nor the M-HF group develop RA hypertrophy, while the HF group had significant RA hypertrophy (HF 0.22±0.02 vs M-HF 0.15±0.01 vs Hypoxia 0.13±0.01) (Figure 2F), indicating that RV dysfunction developed in the HF group but not in the hypoxia or M-HF groups.

LV and RV hemodynamics in the control group, the TAC-induced M-HF or HF groups, and the hypoxia group are presented in Figure 2G–L and Table S3. Both the M-HF and HF groups had significant increases in LV systolic pressure. As compared to the M-HF group, the HF group had a significantly smaller increase in LV systolic pressure (Figure 2G), reaffirming reduced LV function in this group. Both the M-HF and HF groups had significant increases in LV end-diastolic pressure (LVEDP), decreased LV contractility, and increased RV systolic pressure. However, these changes were more significant in the HF group (Figure 2H–L). The TAC-induced HF group also had a significant increase in RV end-diastolic pressure. The RA hypertrophy in this group is consistent with the increased RV end-diastolic pressure and the occurrence of ascites in some of the mice. As expected, the hypoxia group had no significant alterations in LV pressure, LVEDP or LV contractility (Figure 2G–I), but had a significant increase in RV systolic pressure and a small but significant increase in RV end-diastolic pressure (Figure 2K,L). The increase in RV pressure in the M-HF or HF groups was similar or greater to that in hypoxia-induced PH (Figure 2K,L), indicating that TAC-induced HF is an effective cause of pulmonary hypertension in mice.

We further determined the degree of RV fibrosis and cardiac myocyte hypertrophy in response to hypoxia, TAC-induced M-HF or TAC-induced HF. Consistent with the severity of RV hypertrophy in the hypoxia and HF groups, histological analysis indicated a significant increase in RV fibrosis (Figure S1A, B) and cardiac myocyte cross-sectional area (Figure S1A, C) in these groups, indicating that both fibrosis and cardiac myocyte hypertrophy contributed to the RV hypertrophy.

The TAC-induced increase in lung weight is not merely the result of pulmonary edema

LV failure often causes significant increases of lung weight and this is a reliable marker for LV dysfunction.^{8,9,12,13} The increases in lung weight are commonly ascribed to pulmonary edema or increased interstitial fluid. To determine whether the increase in lung weight was a result of pulmonary edema, we determined the relative water content of lung tissue in the sham group, M-HF group and HF group. Surprisingly, while the TAC-induced HF group had a ~3 fold increase in lung weight, this was not the result of increased water content in the lung tissue (Figure 3A). This observation was highly reproducible in the TAC-induced HF model, but contradicts the accepted concept of chronic congestion in heart failure.

TAC-induced HF causes profound lung vascular remodeling and lung fibrosis

We further determined the percentage of non-muscularized (NM), partially muscularized (PM), and fully muscularized small arteries (FM) in mice under control conditions, after TAC-induced M-HF or HF, and after 3 weeks of hypoxia. TAC-induced M-HF or HF and hypoxia all caused increases in fully muscularized small arteries, but these increases were greater in the TAC-induced HF group than in the hypoxia or M-HF groups (Figure 3B). The M-HF, HF and hypoxia groups all had significant decreases in non-muscularized small arteries but these decreases were significantly greater in the HF group than in the other two groups (Figure 3B), indicating that TAC-induced HF is a highly effective model in causing PH and pulmonary vascular remodeling.

Interestingly, the HF group showed prominent pulmonary vascular and perivascular remodeling as indicated by marked vascular wall thickening and vascular lesions (Figure 4, Figure S2–5). The HF group also showed thickened alveolar septa (Figure S2–4) and focal collapsed alveolar airspaces filled with fibroblasts (Figure S4,5), collagen (Figure 4, Figure S6–8), and leucocytes (Figure 5A–C). Staining for smooth muscle α -actin was increased in the area with fibrosis (Figure S4), as in the lung vessels (Figure S4–5), in the HF group, indicating proliferation of smooth muscle cells and myofibroblasts. As compared with

control and M-HF groups, the HF group also showed prominent vascular and perivascular fibrosis (Figure 4A–H) and broadly diffused lung collagen deposition in all of the HF mice (Figure S6, Figure 4D), together with patches of lung fibrosis in some of HF mice (Figure 4C,E,I–K). In addition, data obtained from the whole lung in 3 HF mice reveal that lung fibrosis and vascular remodeling are common phenomena throughout the entire lung.

Lung fibrosis, vascular fibrosis and myofibroblast proliferation are often associated with increased TGF- β signaling. In support of an increase in lung TGF- β signaling in HF mice, TGF- β mRNA was significantly increased in the TAC-induced HF group. However, the increase in TGF- β mRNA was similar between the hypoxia group and the TAC-induced HF group (Figure S9A). Western blot showed that TGF- β protein content was also increased in the M-HF and HF groups (Figure 6A,B). Consistent with the observed interstitial lung fibrosis, real-time quantitative PCR showed that both hypoxia and TAC-induced HF caused increases in lung collagen I and collagen III (Figure S9B–C), but these increases were markedly greater in the TAC-induced HF group than in the hypoxia group (Figure S9). Western blot showed that collagen I and collagen III protein contents were also increased in the M-HF and HF groups (Figure 6A,C,D).

HF causes lung inflammation

Histological analysis demonstrated accumulation of leukocytes and macrophages in the alveoli, inside the vessels, in the vascular wall of large vessels and in the interstitial space of lung tissues obtained from the TAC-induced HF group (Figure 5A–C). The increased infiltration of macrophages was confirmed by staining with macrophage-specific marker Mac-2 (Figure 5B), while the infiltration of neutrophils was confirmed using a specific antibody against mouse neutrophil clone 7/4 (Figure 5C).¹⁴

In addition, the mRNA of the proinflammatory cytokines TNF1 α , MCP-1, TLR 4 were all increased in lung tissues from the hypoxia, M-HF and HF groups, and these increases were markedly greater in the TAC-induced HF group than in the other groups (Figure S9D–F). IL-1 β , VCAM and ICAM-1 were all increased in lung tissues from the hypoxia, M-HF and HF groups, but the increases were similar (Figure S9G–I). Western blots showed that TNF1 α , ICAM and VCAM protein contents were also increased in M-HF and HF groups (Figure 6A, E–G).

Discussion

Here we report massive pulmonary fibrosis, vascular remodeling, type-2 PH and right ventricular dysfunction in response to LV systolic pressure overload produced by chronic transverse aortic constriction in mice. Strikingly, the dramatic increase of lung weight in mice four weeks after TAC, with severe LV dysfunction, was not the result of an increase of lung water but was associated with massive lung fibrosis, leukocyte infiltration and profound vascular remodeling. This observation was highly reproducible in the TAC-induced HF model, but is contrary to the accepted concept of pulmonary edema or congestion in chronic heart failure. The prominence of lung fibrosis in this model may provide novel insights regarding the progression of, and clinical treatment for, end-stage LV dysfunction. The lung fibrosis and remodeling may be an important mechanism for the poor clinical outcome in patients of end-stage heart failure. Thus, the effective treatment of LV end-stage heart failure may also require additional efforts to reduce lung fibrosis and inflammatory response.

The increase in LV after-load caused by TAC leads to pathologic LV hypertrophy, a decrease in LV ejection fraction and an increase in LV end-diastolic pressure. The increased LV filling pressure resulted in impressive LA hypertrophy, an increase in pulmonary artery

pressure, right ventricular (RV) hypertrophy, and RV dysfunction, as indicated by increased RV end-diastolic pressure and RA hypertrophy. TAC-induced LV dysfunction also caused a dramatic increase in the percentage of fully muscularized small pulmonary arteries, marked lung fibrosis, myofibroblast proliferation, and leukocyte infiltration. The potential mechanism of TAC-induced pulmonary remodeling and mortality is summarized in Figure 6H. These changes mirror the histological remodeling described in human pulmonary venous hypertension secondary to mitral stenosis, and left ventricular failure.¹⁵⁻¹⁷

The massive lung fibrosis in this type-2 PH model suggests that an effective treatment of LV end-stage heart failure may require additional efforts to reduce lung fibrosis. In the context of the poor clinical outcome for patients with lung fibrosis, the mission to treat lung fibrosis in type-2 PH model can be very challenging. A team effort from experts in the field of heart failure, pulmonary hypertension and lung fibrosis is likely to be required to achieve optimal treatment of congestive heart failure. Moreover, the considerable lung fibrosis may be an important mechanism for the poor clinical outcome in patients with end-stage heart failure.

Given the important role for TGF-1 β in lung fibrosis, vascular fibrosis and fibroblast proliferation, increased lung TGF-1 β mRNA and protein contents in heart failure mice suggest that the TGF-1 β signaling pathway might contribute to the development of lung fibrosis and remodeling in this model. Whether disruption of the TGF-1 β signaling pathway can attenuate the development of lung fibrosis requires further careful investigation.

The pulmonary vascular remodeling, PH and RV hypertrophy caused by TAC-induced LV failure was greater than that produced by hypoxia (10% oxygen exposure). The increases in lung TGF-1 β , TNF α , MCP-1, IL-1 β , TLR-4, ICAM (Intercellular Adhesion Molecule-1) and VCAM (Vascular Cell Adhesion Molecule-1) mRNA or protein content, that have been previously observed in hypoxia-induced PH mice, were also observed in lung tissues from mice with TAC-induced PH. These data indicate that TAC-induced type 2 PH model shares some characteristics in common with those observed in hypoxia-induced PH in mice. Since ICAM and VCAM facilitate leukocyte-endothelial interaction and leukocyte infiltration, the increased lung ICAM and VCAM protein in TAC-induced PH mice might be partially responsible for the increased lung leukocyte infiltration. The prominent lung inflammatory response in this type-2 PH model suggests that attenuation of lung inflammation may be a potentially useful approach to treat heart failure and type-2 PH.

There are two major limitations for our study. First, although we have not observed any evidence of an increase of lung water content in any of our heart failure mice (mice with either moderate or severe LV dysfunction), it is not clear whether there may have been transient lung edema earlier in the development of the model. Second, the mouse TAC-induced PH model is relatively acute compared to the more chronic course observed in patients with mitral stenosis or left ventricular failure. Therefore, this mouse model may not fully mimic the clinical type-2 PH. Nevertheless, similar histological findings have been described in the clinical situation suggesting that the TAC-induced PH mouse model is clinically relevant. Moreover, given that thousands of genetically modified mouse strains are currently available, and thousands of tissue-specific gene knockout or knockin mouse strains will become available, the TAC-induced PH mouse model is likely to be a valuable tool to explore molecular mechanisms or novel therapeutic approaches for type-2 PH.

Perspectives

Pulmonary hypertension (**PH**) secondary to chronic left ventricular failure is classified as type-2 PH. It is predicted that up to 60% of patients with severe LV systolic dysfunction and up to 70% of patients with LV diastolic dysfunction may develop PH. Understanding the

molecular mechanisms for type-2 PH and the development of novel treatments for this condition requires a robust experimental animal model and a good understanding of the nature of the resultant pulmonary remodeling. Here we demonstrate that pressure overload produced by transverse aortic constriction causes up to 5.3-fold increase in lung wet weight and dry weight, massive pulmonary fibrosis, and type-2 PH in mice. Interestingly, the pressure overload-induced increase in lung weight was not associated with pulmonary edema, but resulted from profound pulmonary remodeling with a dramatic increase in the percentage of fully muscularized lung vessels, marked vascular and lung fibrosis, and leukocyte infiltration. The considerable lung fibrosis, leukocyte infiltration and PH in mice after pressure overload, mimic findings in clinical mitral stenosis and clearly indicate that pulmonary venous hypertension also causes severe lung disease. The massive lung fibrosis may be an important mechanism in the poor clinical outcome in patients with end-stage heart failure. Our findings suggest that the effective treatment of LV end-stage heart failure may require significant efforts to reduce lung fibrosis and inflammation.

Supplementary Material

Refer to Web version on PubMed Central for supplementary material.

Acknowledgments

None.

Sources of Funding This study was supported by U.S. Public Health Service Grants R21HL098669, R21HL098719, R21HL102597, RO1HL105406, 1RO1 HL079168 and RO1HL65322 from NIH, and VA Research funding.

Reference

1. Simonneau G, Robbins IM, Beghetti M, Channick RN, Delcroix M, Denton CP, Elliott CG, Gaine SP, Gladwin MT, Jing ZC, Krowka MJ, Langleben D, Nakanishi N, Souza R. Updated clinical classification of pulmonary hypertension. *J Am Coll Cardiol*. 2009; 54(1 Suppl):S43–54. [PubMed: 19555858]
2. Cournand A, Bloomfield RA, Lauson HD. Double lumen catheter for intravenous and intracardiac blood sampling and pressure recording. *Proc Soc Exp Biol Med*. 1945; 60:73–75. [PubMed: 21004035]
3. Galié N, Hoepfer MM, Humbert M, Torbicki A, Vachiery JL, Barbera JA, Beghetti M, Corris P, Gaine S, Gibbs JS, Gomez-Sanchez MA, Jondeau G, Klepetko W, Opitz C, Peacock A, Rubin L, Zellweger M, Simonneau G. Guidelines for the diagnosis and treatment of pulmonary hypertension. *Eur Respir J*. 2009; 34:1219–1263. [PubMed: 19749199]
4. Hoepfer MM, Barberá JA, Channick RN, Hassoun PM, Lang IM, Manes A, Martinez FJ, Naeije R, Olschewski H, Pepke-Zaba J, Redfield MM, Robbins IM, Souza R, Torbicki A, McGoon M. Diagnosis, assessment, and treatment of non-pulmonary arterial hypertension pulmonary hypertension. *J Am Coll Cardiol*. 2009; 54(1 Suppl):S85–96. [PubMed: 19555862]
5. Grigioni F, Potena L, Galié N, Fallani F, Bigliardi M, Coccolo F, Magnani G, Manes A, Barbieri A, Fucili A, Magelli C, Branzi A. Prognostic implications of serial assessments of pulmonary hypertension in severe chronic heart failure. *J Heart Lung Transplant*. 2006; 25:1241–1246. [PubMed: 17045937]
6. Ghio S, Gavazzi A, Campana C, Inserra C, Klersy C, Sebastiani R, Arbustini E, Recusani F, Tavazzi L. Independent and additive prognostic value of right ventricular systolic function and pulmonary artery pressure in patients with chronic heart failure. *J Am Coll Cardiol*. 2001; 37:183–188. [PubMed: 11153735]
7. Lu Z, Fassett J, Xu X, Hu X, Zhu G, French J, Zhang P, Schnermann J, Bache RJ, Chen Y. Adenosine A3 receptor deficiency exerts unanticipated protective effects on the pressure-overloaded left ventricle. *Circulation*. 2008; 118:1713–1721. [PubMed: 18838560]

8. Lu Z, Xu X, Hu X, Lee S, Traverse JH, Zhu G, Fassett J, Tao Y, Zhang P, dos Remedios C, Pritzker M, Hall JL, Garry DJ, Chen Y. Oxidative stress regulates left ventricular PDE5 expression in the failing heart. *Circulation*. 2010; 121:1474–1483. [PubMed: 20308615]
9. Xu D, Guo H, Xu X, Lu Z, Fassett J, Hu X, Xu Y, Tang Q, Hu D, Somani A, Geurts AM, Ostertag E, Bache RJ, Weir EK, Chen Y. Exacerbated pulmonary arterial hypertension and right ventricular hypertrophy in animals with loss of function of extracellular superoxide dismutase. *Hypertension*. 2011; 58:303–309. [PubMed: 21730301]
10. Lu Z, Xu X, Hu X, Zhu G, Zhang P, van Deel ED, French JP, Fassett JT, Oury TD, Bache RJ, Chen Y. Extracellular superoxide dismutase deficiency exacerbates pressure overload-induced left ventricular hypertrophy and dysfunction. *Hypertension*. 2008; 51:19–25. [PubMed: 17998475]
11. Urboniene D, Haber I, Fang YH, Thenappan T, Archer SL. Validation of high-resolution echocardiography and magnetic resonance imaging versus high-fidelity catheterization in experimental pulmonary hypertension. *Am J Physiol Lung Cell Mol Physiol*. 2010; 299:L401–L412. [PubMed: 20581101]
12. Lu Z, Xu X, Hu X, Fassett J, Zhu G, Tao Y, Li J, Huang Y, Zhang P, Zhao B, Chen Y. PGC-1 α regulates expression of myocardial mitochondrial antioxidants and myocardial oxidative stress after chronic systolic overload. *Antioxid Redox Signal*. 2010; 13:1011–1022. [PubMed: 20406135]
13. Takimoto E, Champion HC, Li M, Belardi D, Ren S, Rodriguez ER, Bedja D, Gabrielson KL, Wang Y, Kass DA. Chronic inhibition of cyclic GMP phosphodiesterase 5A prevents and reverses cardiac hypertrophy. *Nat Med*. 2005; 11:214–222. [PubMed: 15665834]
14. Wang H, Zhang W, Tang R, Hebbel RP, Kowalska MA, Zhang C, Marth JD, Fukuda M, Zhu C, Huo Y. Core2 1-6-N-glucosaminyltransferase-I deficiency protects injured arteries from neointima formation in ApoE-deficient mice. *Arterioscler Thromb Vasc Biol*. 2009; 29:1053–1059. [PubMed: 19372458]
15. Wagenvoort, C.; Wagenvoort, N. *Pulmonary Venous Hypertension*. John Wiley & Sons; New York: 1977. Pathology of Pulmonary Hypertension; p. 177-216.
16. Wagenvoort, CA. Lung biopsies and pulmonary vascular disease. In: Weir, EK.; Reeves, JT., editors. *Pulmonary Hypertension*. Futura Publishing Co; New York: 1984.
17. Haworth SG, Hall SM, Panja M. Peripheral pulmonary vascular and airway abnormalities in adolescents with rheumatic mitral stenosis. *Int J Cardiol*. 1988; 18:405–416. [PubMed: 3360524]

Novelty and Significance

What Is New?

- Chronic pressure overload produced by TAC causes a dramatic increase of lung weight, massive pulmonary fibrosis, leukocyte infiltration, and type-2 PH in mice.
- • The increase of lung weight in mice with chronic heart failure was not the result of an increase of lung water content.

What Is Relevant?

- The massive lung fibrosis, leukocyte infiltration and PH in mice after TAC indicate that chronic systemic hypertension causes severe lung and pulmonary vascular disease.

Summary

- Chronic heart failure causes severe lung disease.
- The effective treatment of end-stage heart failure may require additional efforts to reduce lung fibrosis and inflammation.

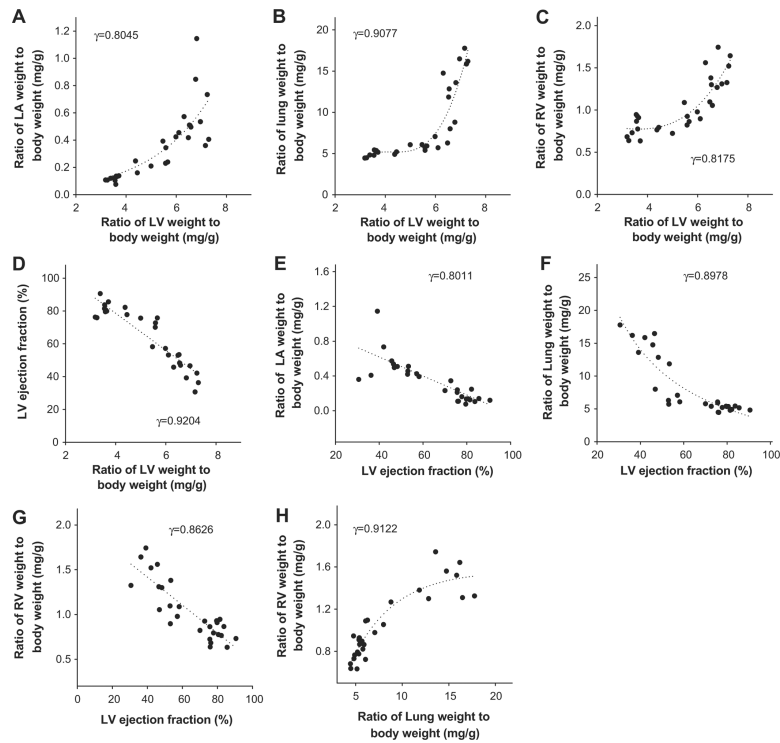


Figure 1. The TAC-induced increases of lung weight and RV hypertrophy are related to the degree of LV hypertrophy and failure

(A–D) Correlations between LV weight and LA weight, lung weight, RV weight or LV ejection fraction; (E–G) Correlations between LV ejection fraction and LA weight, lung weight, or RV weight; (H) correlation between increase of lung weight and RV weight.

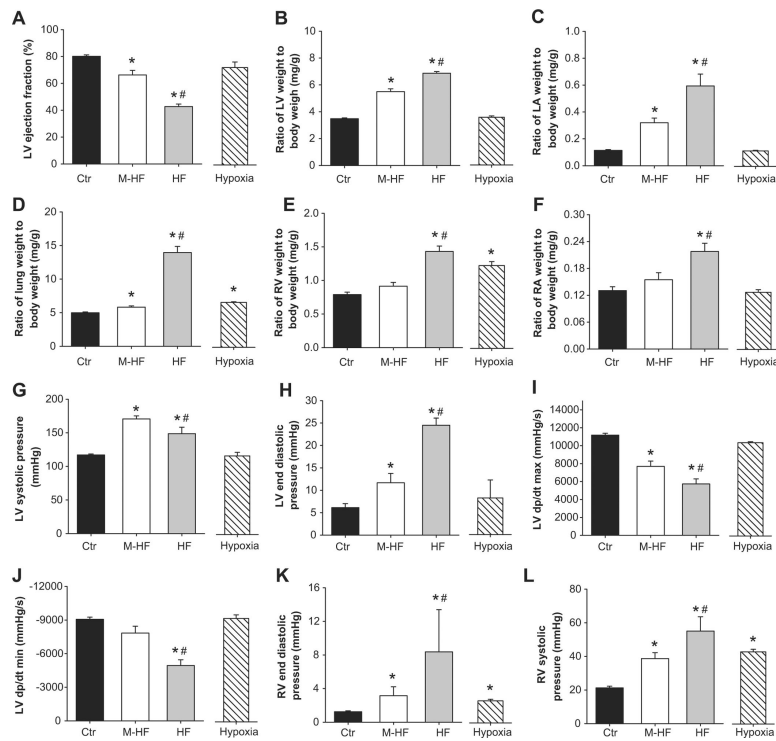


Figure 2. Alterations of heart and lung anatomic data and cardiac function in four experimental groups

(A) LV ejection fraction in each group; (B) Relative LV hypertrophy, (C) LA hypertrophy, (D) increase of lung weight, (E) RV hypertrophy, and (F) RA hypertrophy; (G) HF group shows reduced LV systolic pressure as compared with M-HF group; (H) HF group shows increased LV end-diastolic pressure as compared with other groups; (I,J) HF group shows reduced LV contractility; (K) M-HF and HF groups show increased end-diastolic RV pressure, and (L) increased RV systolic pressure. * $p < 0.05$ vs control group; # $p < 0.05$ vs. corresponding M-HF group.

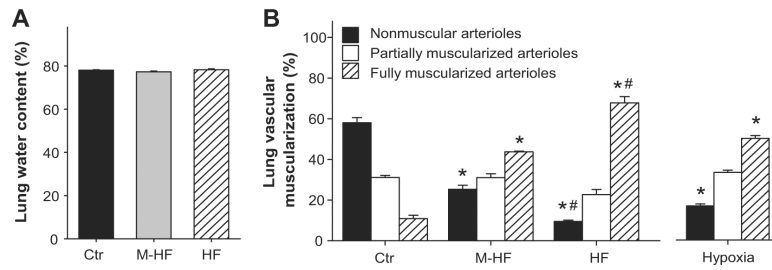


Figure 3. Chronic TAC and hypoxia cause no pulmonary edema, but cause pulmonary vascular remodeling

(A) Chronic TAC-induced increase of lung weight is not related to pulmonary edema or water retention; (B) Distribution of nonmuscular, partially muscular, and fully muscularized small arteries in mice after chronic hypoxia or TAC-induced M-HF and TAC-induced HF.

* $p < 0.05$ vs control group; # $p < 0.05$ vs. corresponding M-HF group.

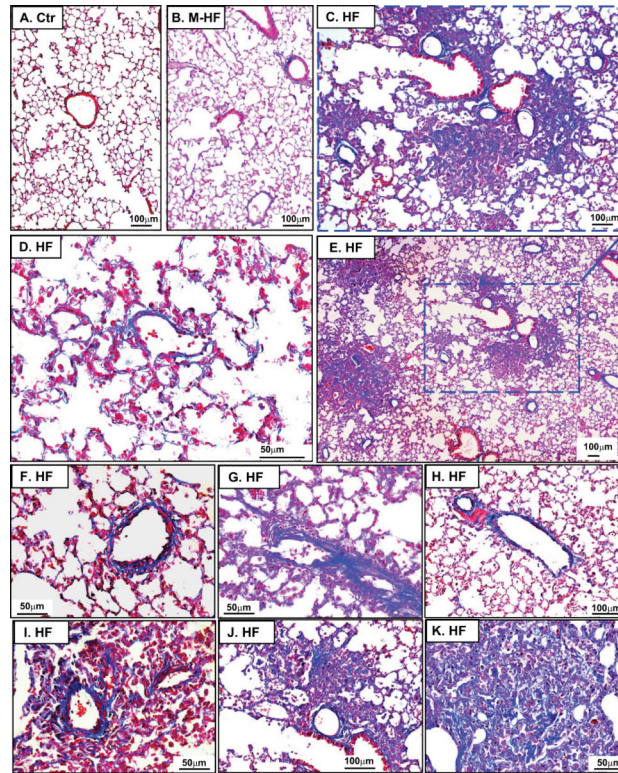


Figure 4. TAC-induced HF causes massive lung fibrosis in mice

Masson's Trichrome staining was used to show the relative collagen deposition (the blue staining) in lung tissues from control (A), M-HF (B) and HF mice (C–K). (B) The general lung structure of M-HF mice is not dramatically changed, but collagen deposition is increased. (C–K) show prominent lung vascular or perivascular fibrosis, and severe focal fibrosis in collapsed lung tissues in HF mice.

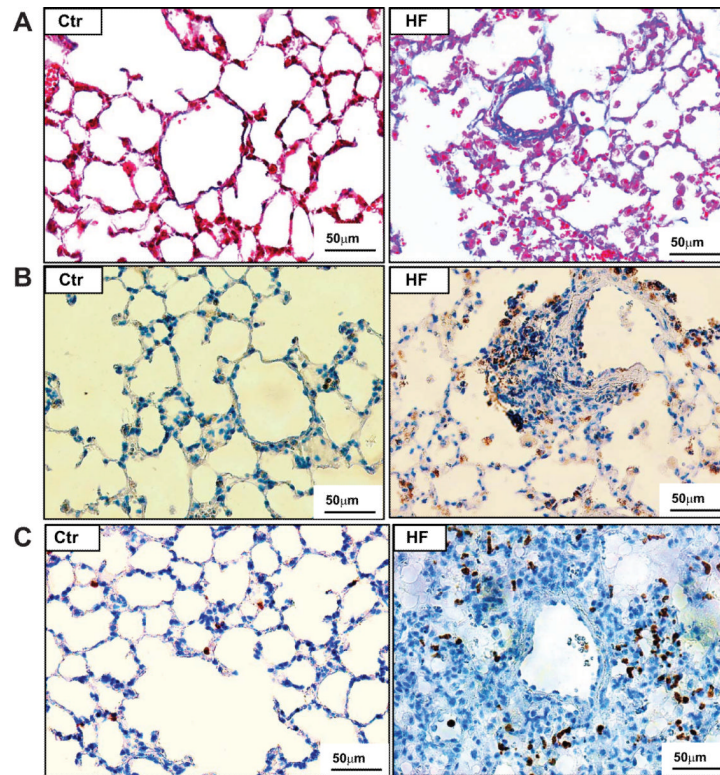


Figure 5. TAC-induced HF causes diffuse lung leukocyte infiltration in mice

(A) Masson's Trichrome staining shows impressive leukocyte infiltration in lung tissues from HF mice compared to controls. (B) The increased infiltration of macrophages was confirmed by staining with macrophage specific marker Mac-2, and (C) the infiltration of neutrophils was confirmed using an antibody specific for neutrophil clone 7/4.

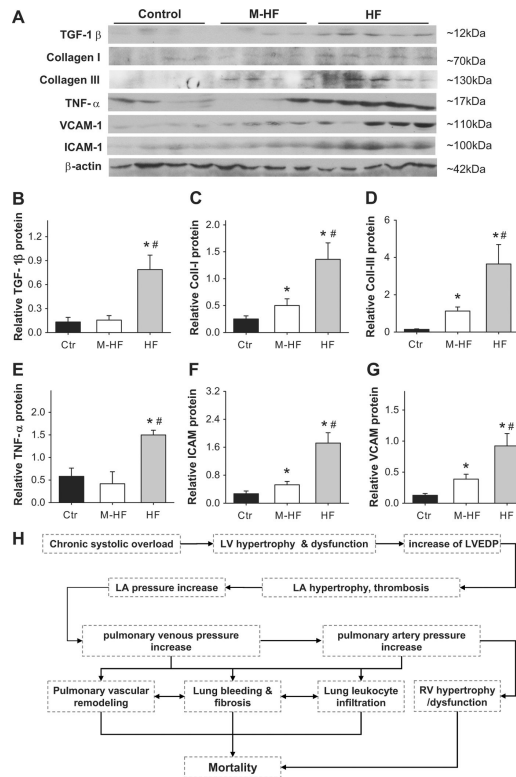


Figure 6. Chronic TAC and hypoxia increased expression of genes related to lung fibrosis and inflammation

(A,B) Expression of TGF-1 β ; (A,C) Collagen-I; (A,D) collagen-III; (A,E) TNF α ; and (A,F,G) adhesion molecules ICAM and VECAM in lung tissues from control group, TAC-induced M-HF or HF groups. (H) The diagram shows the potential mechanism of TAC-induced pulmonary remodeling, pulmonary hypertension and mortality. * $p < 0.05$ vs control group; # $p < 0.05$ vs. corresponding M-HF group.